
Energy-efficient Knowledge Distillation for Spiking Neural Networks

Dongjin Lee¹ Seongsik Park^{1,2} Jongwan Kim^{1,3} Wuhyeong Doh¹ Sungroh Yoon^{1,2,3,4*}

¹Department of Electrical and Computer Engineering

²Institute of New Media and Communications

³Interdisciplinary Program in Artificial Intelligence

⁴Automation and Systems Research Institute

Seoul National University

{ldj9510, pss015, jongwankim, whdoh96, sryoon}@snu.ac.kr

Abstract

Spiking neural networks (SNNs) have been gaining interest as energy-efficient alternatives of conventional artificial neural networks (ANNs) due to their event-driven computation. Considering the future deployment of SNN models to constrained neuromorphic devices, many studies have applied techniques originally used for ANN model compression, such as network quantization, pruning, and knowledge distillation, to SNNs. Among them, existing works on knowledge distillation reported accuracy improvements of student SNN model. However, analysis on energy efficiency, which is also an important feature of SNN, was absent. In this paper, we thoroughly analyze the performance of the distilled SNN model in terms of accuracy and energy efficiency. In the process, we observe a substantial increase in the number of spikes, leading to energy inefficiency, when using the conventional knowledge distillation methods. Based on this analysis, to achieve energy efficiency, we propose a novel knowledge distillation method with heterogeneous temperature parameters. We evaluate our method on two different datasets and show that the resulting SNN student satisfies both accuracy improvement and reduction of the number of spikes. On MNIST dataset, our proposed student SNN achieves up to 0.09% higher accuracy and produces 65% less spikes compared to the student SNN trained with conventional knowledge distillation method. We also compare the results with other SNN compression techniques and training methods.

1 Introduction

Energy consumption has become a major concern of deep learning as large-scale artificial neural networks (ANNs), such as self-attention models [33], have shown notable achievements. Due to the recent trend of energy consumption, ANN compression has become an essential process not only in resource-constrained environments, but also in server computers. The compression methods, including quantization [10, 12], pruning [9], and knowledge distillation [11], have been actively studied and successfully improved the energy efficiency of ANNs.

As another approach to reducing the energy consumption, there have been attempts to introduce spiking neural networks (SNNs), which aim to mimic the behavior of the human brain. SNNs are considered the next generation of ANNs [19] and especially, promising on neuromorphic architectures [6, 21]. Thanks to the high energy efficiency, it is expected that SNNs can be deployed on resource-restricted environments, such as robots [36] and drones [34].

*corresponding author

To achieve a significant improvement in the energy efficiency with compressed SNNs, the above two approaches have been combined [5, 7, 25]. For successful deployment to neuromorphic chips, this integration in deep SNNs is inevitable and more important than in ANNs. However, most of the studies, unlike those of ANNs, have focused on quantization [1, 27, 29, 39] and pruning [20, 30] in deep SNNs. This is because knowledge distillation indispensably requires training procedure, which is challenging in deep SNNs. This hinders broader applicability of deep SNNs.

The training of deep SNNs is challenging because of complex neuronal dynamics and non-differentiable spiking function, which restrict exploiting ANNs' successful training algorithms, such as stochastic gradient descent (SGD) and error backpropagation. To address these obstacles, recently, direct training methods for deep SNNs have been proposed [31, 37, 41]. These approaches mainly use surrogate gradients or models instead of the non-differentiable function to apply SGD and error backpropagation. Several studies have shown comparable results to ANNs with the direct training method [42]. The recent development in training algorithms of SNNs provides opportunities for introducing knowledge distillation into deep SNNs. There have been a few studies about knowledge distillation [16, 35], but they have shown insufficient results on accuracy and have not consider the efficiency of SNNs, such as the number of spikes.

In this paper, to improve both training performance and efficiency, we adopt knowledge distillation to SNNs. As one of the early-stage studies of knowledge distillation on SNNs, we investigate the performance of conventional approaches in terms of accuracy and the number of spikes, which are both crucial metrics for energy-efficient SNNs. According to our analysis, the conventional methods, originally designed without assuming the use in SNNs, could not fully bring out the best performance and resulted in the increase of the number of spikes in the student models. Based on the in-depth analysis, we propose an energy-efficient knowledge distillation method dedicated for SNNs. In the proposed approach, heterogeneous temperatures are used during distillation to reduce the number of spikes in the student model. By applying our method, we could achieve accurate and efficient SNNs. To the best of our knowledge, this work is the first attempt to take energy efficiency into account when applying knowledge distillation to SNNs. The contributions of this paper can be summarized as follows:

- **In-depth analysis of knowledge distillation on SNNs:** We thoroughly analyze the effect of knowledge distillation on deep SNNs.
- **Significant improvement in energy efficiency:** We propose energy-efficient knowledge distillation on deep SNNs, which greatly reduced the number of spikes in the student model, compared to conventional methods.

2 Background

2.1 Spiking neural networks

SNNs are biologically plausible neural networks which mimic the event-driven computation of human brain. The biological plausibility of SNNs comes from their spiking neurons, the elementary processing units in SNNs which transfer information through binary spike trains. Integrate-and-fire (IF) neuron is one of the most widely used spiking neurons in SNNs, which mimics the integration and firing mechanism of action potentials in human brain. IF neuron integrates synaptic inputs from presynaptic neurons and fires a spike when its membrane potential exceeds a certain threshold value. The dynamics of IF neuron can be formulated as follows:

$$u_j^l(t) = u_j^l(t-1) + z_j^l(t), \quad (1)$$

where $u_j^l(t)$ is a membrane potential of j th neuron in l th layer. $z_j^l(t)$ is a sum of synaptic inputs from presynaptic neurons, which can be described as follows:

$$z_j^l(t) = \sum_i w_{ij}^l S_i^{l-1}(t) + b_j^l, \quad (2)$$

where w_{ij}^l is a synaptic weight and b_j^l is a bias. $S_i^{l-1}(t)$ represents spike trains from presynaptic neuron i satisfying the firing condition which is stated as

$$S_i^{l-1}(t) = \sum_{t_i^{l-1,(f)} \in F_i^{l-1}} \delta(t - t_i^{l-1,(f)}), \quad (3)$$

where $\delta(t)$ is the Dirac delta function and F_i^{l-1} is a set of firing times satisfying the firing condition, represented by

$$F_i^{l-1} = \{t_i^{l-1,(f)} | u_i^{l-1}(t_i^{l-1,(f)}) \geq v_{\text{th}}\}. \quad (4)$$

Due to the discrete firing mechanism using spikes as mentioned above, SNNs operate in an event-driven fashion, which has an advantage in energy efficiency [28]. However, considering deployment to constrained neuromorphic devices, downsizing SNN models has become a necessary task. In this flow, several works have applied various compression techniques, originally used for ANNs, to SNNs. [30] proposed soft-pruning during training of SNNs which significantly reduced the number of weight updates. [20] applied pruning to SNN models with voice activity detection task, removing 85% of the network connections without performance loss. There also have been many studies that focused on applying quantization to SNNs. [29] downsized SNN models by 73.78% with low-precision parameters at the cost of 1.04% test error increase. Other works showed potential of low-precision SNNs on various object recognition datasets [1, 27, 39].

However, the abovementioned research did not fully consider metrics crucial in SNNs such as inference latency and energy efficiency. This lack can lead to redundant latency with over-spikes. Since synaptic operations are dominant power consumers on neuromorphic devices [32], these models might face limitations when it comes to using SNNs in power-constrained environments. [7] applied weight quantization and pruning to reduce the model complexity of SNNs, without losing much functionality. In addition, they suggested activity regularization method to reduce the spike events. [22, 32] included regularization term in loss function to restrict the number of fired spikes, which improved the energy efficiency of SNNs. [18] applied binary quantization on SNNs with careful selection of spiking neuron dynamics considering the number of operations. [25] suggested STDP-based pruning with quantization to efficiently compress SNN models. [5] proposed spatial and temporal pruning and weight quantization for low-latency, highly efficient SNNs. These works satisfied both model size reduction and energy efficiency of SNNs, which is the desirable direction for SNN compression.

2.2 Knowledge distillation

Efficiently transferring knowledge from large teacher network to small student network has been a traditional topic which has drawn more and more attention in recent years. Adopting this teacher-student learning paradigm, many distillation methods have been investigated. [2] first proposed model compression that transfers information from a large model or from an ensemble of models to a small model without a significant drop in accuracy. [11] proposed the concept of soft label which is distilled from the teacher model to the student model. Soft labels are the probabilities of an input belonging to each class, and can be estimated by a softmax function. Here, a temperature factor is introduced to control the importance of each soft label, which contains the informative dark knowledge from the teacher model. By increasing the temperature, the logits can contain richer information than one-hot labels. However, if the temperature becomes too large, the probability of irrelevant classes will also be over-emphasized.

Extra information other than the outputs, for example, the intermediate-level supervision from the teacher model, can additionally boost the performance of knowledge distillation. Application of the intermediate representations was first introduced in FitNet [26] to provide hints to improve the training of the student model. Thanks to the additional hint-based training, the trained deep student network showed better accuracy with fewer parameters compared to the original wide teacher network. To explore the relationships between different feature maps, [40] proposed a flow of solution process (FSP), which is defined by the Gram matrix between two layers. Many other different algorithms have been proposed to improve the process of distilling knowledge in more complex settings. [3, 15, 38, 41]

As mentioned above, knowledge distillation has been extensively studied and effectively used for ANNs in the literature. However, some recent works show how off-the-shelf knowledge distillation commonly used in ANNs can be adapted for SNNs. [16] first proposed a study that applied knowledge distillation to SNNs. In this work, output spike train of the teacher SNN model was involved in the distillation process, but the performance was unsatisfactory. [35] proposed knowledge distillation for an SNN model obtained by first training an ANN model and then copying the weights to the SNN model, which is the process called ANN-to-SNN conversion. Both of the previous studies share the same base as [11] in that knowledge is distilled to the student model using the outputs. The study of knowledge distillation on SNNs is still at an early stage, and for this reason, the simple but effective

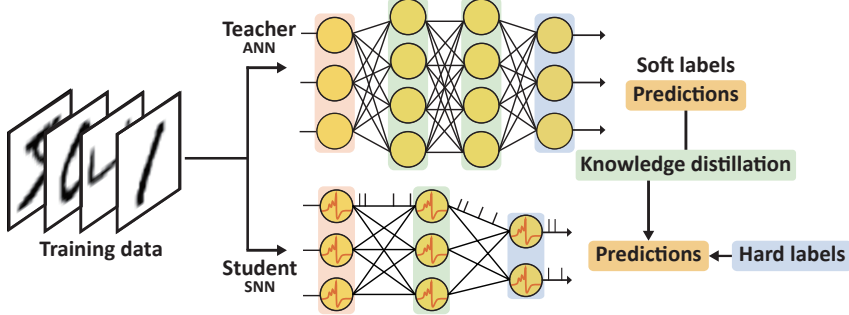


Figure 1: Overview of the knowledge distillation method for SNNs.

method of [11], which was an early-stage study of knowledge distillation, has been widely adopted in SNNs.

3 Methodology

3.1 Analyzing conventional knowledge distillation applied to SNNs

As already mentioned in the previous section, knowledge distillation has been conventionally applied to SNN models based on the method proposed in [11]. The overall process of knowledge distillation in SNNs is visualized in Fig. 1. In this method, the loss term is formulated as

$$L = \alpha L_{CE} + (1 - \alpha)L_{KD}, \quad (5)$$

where L_{CE} is the original cross entropy loss, L_{KD} is additional distillation loss, and the two loss terms are balanced by a weighting hyperparameter α . Moreover, L_{KD} can be computed as

$$L_{KD} = \tau^2 D_{KL}(\sigma(z^s; T = \tau) || \sigma(z^t; T = \tau)), \quad (6)$$

where Kullback Leibler divergence is adopted, and temperature T with $\tau > 1$ is used to soften the output logits of the student and the teacher, notated z^s and z^t respectively. The softened output logits are normalized by a softmax function $\sigma(\cdot)$, which can be described by

$$\sigma(z_k; T = \tau) = \frac{e^{z_k / \tau}}{\sum_i e^{z_i / \tau}}. \quad (7)$$

The performance of knowledge distillation depends on the choices of the two hyperparameters, T and α . In past studies, T and α have been commonly decided in a heuristic manner, usually following the popular choices [4], to derive only the best inference accuracy. [16, 35] However, when applying knowledge distillation to SNNs, both accuracy and energy efficiency should be considered together as important metrics when evaluating the performance of the models. Accordingly, in this paper we first investigate the performance of knowledge distillation in SNN models in terms of inference accuracy and energy efficiency by changing the values of T and α . For energy efficiency, we measure the number of spikes occurring inside the network, which serves as an effective indicator for estimating energy efficiency. A baseline SNN model trained from scratch is also evaluated in the same way for fair comparison.

From the aforementioned analysis, we find that the hyperparameter sets that lead to student SNN models with high accuracy also result in the increase in the number of spikes, which will be described in detail in Section 4.2. This can act as a major drawback when trying to apply knowledge distillation to SNNs, as the number of spikes is strongly related to the energy efficiency of the model. To address this issue, we conduct a second analysis on the weight and output distributions to determine the cause for this increase. The related results can be found in Section 4.3.

3.2 Knowledge distillation with heterogeneous temperature

We come to the conclusion that the temperature is the key factor, which has been conventionally applied to both the teacher and the student outputs with the same value without doubt, as in Eq.6.

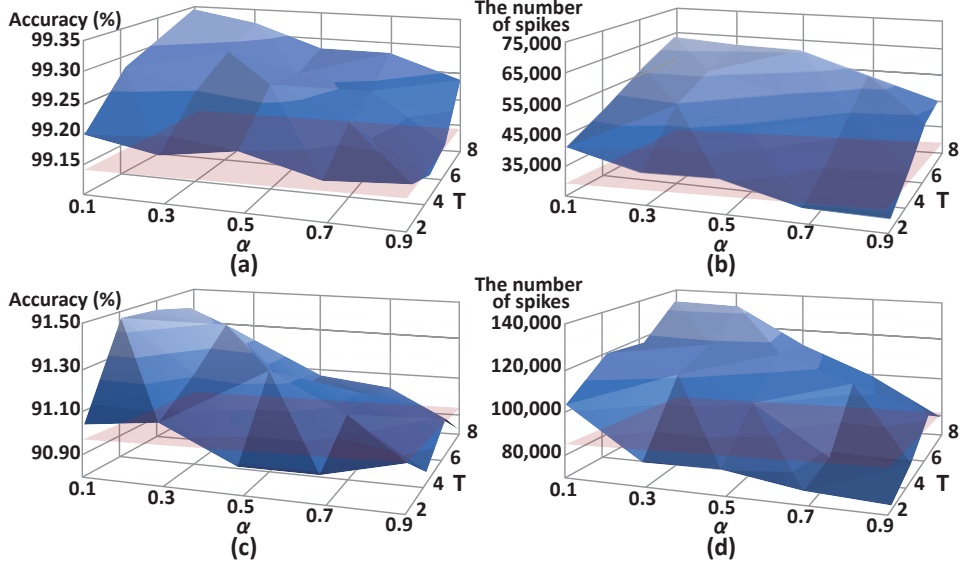


Figure 2: Experimental results on the (MNIST, Fashion-MNIST) datasets according to various configurations of T and α : (a), (c) accuracy and (b), (d) the number of spikes. The red plane represents the results of the baseline.

However, we find that in SNNs, T applied to the teacher output and T applied to the student output play different roles in the distilling process. With this in mind, we propose a novel knowledge distillation method that significantly reduces the number of spikes while boosting the inference accuracy of the student SNN models when compared with the conventional method.

We construct a new loss term by introducing heterogeneous temperatures for the outputs of student and teacher models. The reformed KD loss L_{KD} is as follows:

$$L_{\text{KD}} = T_s T_t D_{\text{KL}}(\sigma(z^s; T = T_s) || \sigma(z^t; T = T_t)), \quad (8)$$

where T_s and T_t are the temperatures applied to the student SNN model and the teacher ANN model, respectively. With this simple change in the loss term, by only tweaking the existing temperature parameter, we can effectively regulate the number of spikes in student SNN models while maintaining their accuracy. Detailed results are covered in the next section.

4 Results

4.1 Experimental settings

We experimented with NVIDIA Titan X (Pascal) GPU and we implement our method with PyTorch framework. We conducted experiments on two standard object classification datasets, MNIST and Fashion-MNIST. For MNIST dataset, we use a pretrained VGG-13 network with batch normalization as the ANN teacher. The shallow student SNN model consists of two convolutional layers and single fully-connected layer. For Fashion-MNIST dataset, we use a pretrained VGG-16 network with batch normalization as the ANN teacher. The student SNN model consists of two convolutional layers and two fully-connected layers. For the training process, we use the Adam optimizer with learning rate of 1e-3. The student SNN models are trained for 10 and 15 time steps, 50 and 100 epochs for MNIST and Fashion-MNIST dataset, respectively. Baseline SNN models, to which knowledge distillation is not applied, are trained with the same networks and parameters. The values shown in the results are the average of 5 repeated experiments. The detailed settings of hyperparameters and networks are shown in Appendix A.

4.2 Analyzing the performance of conventional knowledge distillation

In this section, we evaluate the performance of the conventional knowledge distillation methods and point out their limitations. Here, the loss from Eq. 5 and 6 are used to train the student SNN models.

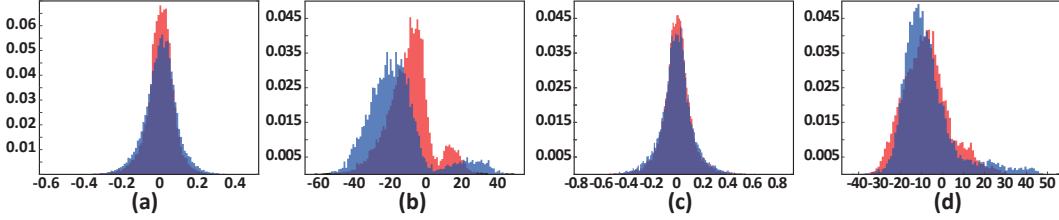


Figure 3: Normalized distributions of: (a), (c) weights in the second convolutional layer of SNN models and (b), (d) outputs over a single batch of test datasets, on (MNIST, Fashion-MNIST) datasets. Baseline and the student SNN model are compared, colored red and blue, respectively.

We verify the impact of temperature and weight parameter on both accuracy and the number of spikes. We increased α by 0.2 increments from 0.1 to 0.9 and T by 2 increments from 2 to 8. The results are shown in Fig. 2. Exact numbers can be found in Appendix B.

Inference accuracy. Fig. 2 (a) and (c) illustrate the inference accuracy of SNN student models trained on the MNIST and Fashion-MNIST dataset respectively with varying temperature T and weight α . From these experiments, we find that the smaller the α , that is, the higher the ratio of L_{KD} , the higher the inference accuracy tends to be. This observation fits well with results from earlier studies [4, 11]. Note that since most of the students showing high accuracy were trained with $\alpha = 0.1$, we fix α as 0.1 for other experiments, which will be outlined in the following sections. We also find that as T increases, the inference accuracy also tends to increase accordingly. In other words, the softness of output logits contribute to accuracy improvement in general. Up to this point, we report the accuracy improvement of the student SNN model through conventional knowledge distillation, which also has been done by other SNN knowledge distillation studies.

The number of spikes. Here, we estimate the energy efficiency of the student SNN models by analyzing the number of spikes they generate during inference of a single image. This process has not been attempted in other SNN knowledge distillation studies, to the best of our knowledge. As in Fig. 2 (b) and (d), the number of spikes shows a similar tendency to the inference accuracy, i.e., smaller α and larger T lead to the considerable increase in the number of spikes. In the experiment with the MNIST dataset for example, the student SNN model with the highest accuracy, trained with $\alpha=0.1$ and $T=8$, generated more than twice the spikes compared to the baseline SNN model. In the following sections, we aim to tackle this unwanted issue of the increase in the number of spikes.

4.3 Why does the number of spikes increase?

As in Eq. 1 and 2, the output membrane potential is the result of the spikes multiplied by the synaptic weights summed over the time steps. Thus it can be inferred that the change in the number of spikes will have any effect on the outputs or the weights. From this hint, we explore the cause of the increase in the number of spikes by observing and comparing the weight and output distributions of the baseline model and the student SNN model.

Fig. 3 (a) and (c) illustrate the weight distributions of the baseline and the student SNN model for the MNIST and Fashion-MNIST dataset. The weight distribution of the second convolutional layer, which has the most parameters, is depicted as a representative. The weight distributions of the rest of the layers are shown in Appendix B. From the figures, we find that the distributions of the two models, which closely resemble Gaussian distributions, look alike. The range is almost the same, yet the variance is slightly higher in the case of the student.

Fig. 3 (b) and (d) illustrate the output distributions of the baseline and the student SNN model. The output logits are derived from a single batch of 1,000 sample input images to form these distributions. As can be seen, the logits from incorrect labels are gathered around the negative area, whereas the logits from correct labels are gathered around the opposite positive area, each cluster resembling a Gaussian distribution. The difference is that the outputs of the distilled student SNN model are more distributed to extremes, or in other words, gathered around larger absolute values than the baseline. Recall that the spikes and the weights are multiplied and aggregated to form the outputs. The weights are similar, but since the outputs are larger, spikes should be generated more accordingly.

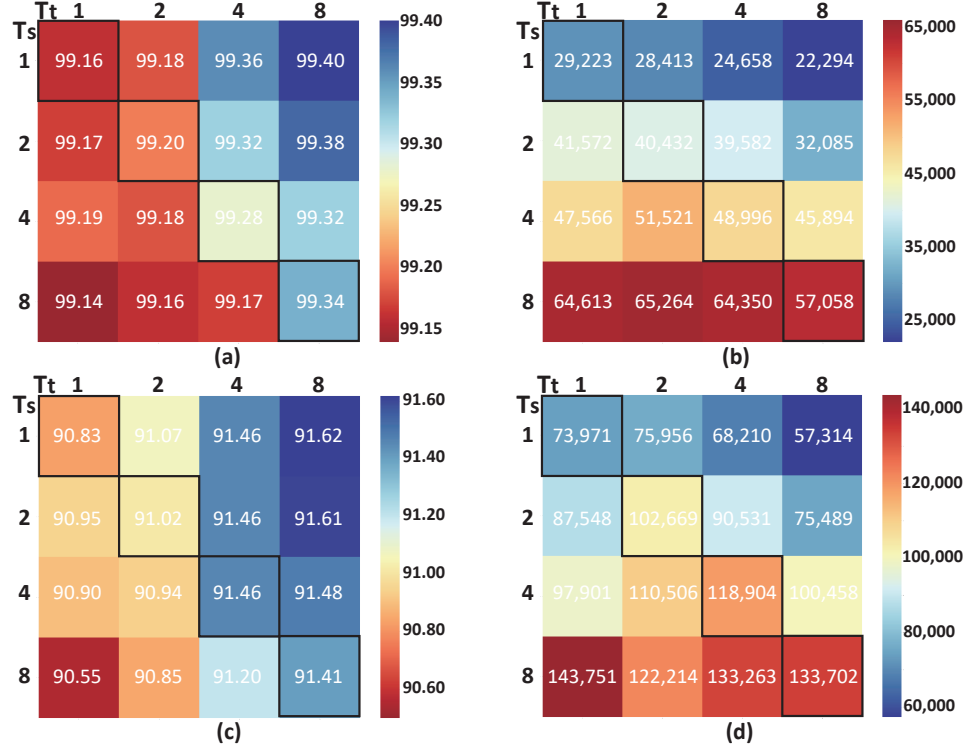


Figure 4: Experimental results expressed as a heatmap on the (MNIST, Fashion-MNIST) datasets according to various configurations of T_s and T_t : (a), (c) accuracy and (b), (d) the number of spikes.

4.4 Analyzing the performance of proposed knowledge distillation

In this section, we evaluate the performance of our knowledge distillation method using heterogeneous temperatures. The loss from Eq. 5 and 8 are used to train the student SNN models. α was fixed at 0.1, and we doubled T_s and T_t from 1 to 8. The distilled results are shown in Fig. 4. The diagonal cells from top left to bottom right are the cases when $T_s = T_t$; thus they are emphasized with borders.

Inference accuracy. Fig. 4 (a) and (c) show the inference accuracy of the student models depending on the two temperature parameters T_s and T_t . The accuracy of the student SNN models tend to increase as T_s gets smaller and T_t gets larger. For the MNIST dataset, the best inference accuracy (99.43%) is obtained with $T_s = 1$ and $T_t = 8$, which is even higher than the previous best (99.34%) with $T_s = T_t = 8$. The same goes for the Fashion-MNIST dataset, where accuracy of heterogeneous temperature $T_s = 1$ and $T_t = 8$ (91.62%) outperforms that of the previous equal temperature $T_s = T_t = 4$ (91.46%).

The number of spikes. The number of spikes vary to a great extent according to the values of T_s and T_t . Opposed to the tendency of inference accuracy, spikes occurred less with small T_s and large T_t , as can be seen in Fig. 4 (b) and (d). The temperature combination $T_s = 1$ and $T_t = 8$, which resulted in the best inference accuracy for the MNIST dataset, also gave the least number of spikes, successfully reducing the over-generated spikes resulted from equal temperature $T_s = T_t = 8$. As high accuracy and low number of spikes are desirable, we can say that distillation with small T_s and large T_t gives the best performance overall.

Table. 1 summarizes the performance of the teacher ANN, baseline SNN, and the student SNN models. The student SNN models trained with knowledge distillation with heterogeneous temperature outperform students trained with standard knowledge distillation. The inference accuracy is improved by 0.09% and 0.16%, and the number of spikes is reduced by 65% and 52% for the MNIST and Fashion-MNIST datasets, respectively. The exact number of spikes and spike frequencies for neurons in each layer can be found in appendix B.

Table 1: Performance comparison between the models on the MNIST and Fashion-MNIST datasets.

Dataset	Model	Accuracy	Number of spikes
MNIST	teacher (ANN)	99.63%	-
	baseline	99.14%	28111
	student (equal T)	99.34%	63184
F-MNIST	student (heterogeneous T)	99.43%	22294
	teacher (ANN)	94.54%	-
	baseline	90.98%	79845
	student (equal T)	91.46%	118904
	student (heterogeneous T)	91.62%	57314

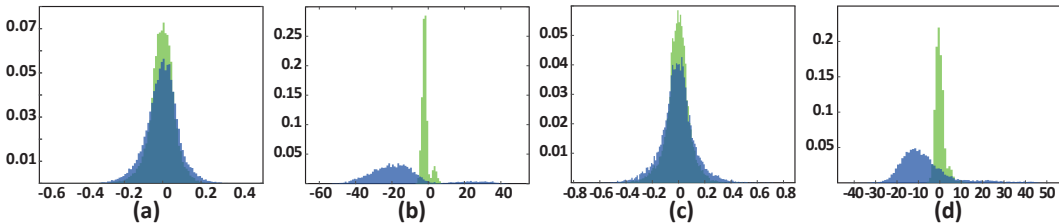


Figure 5: Normalized distributions of: (a), (c) weights in the second convolutional layer of SNN models and (b), (d) outputs over a single batch of test datasets, on (MNIST, Fashion-MNIST) datasets. The student SNN models with equal/heterogeneous T are compared, colored blue and green, respectively.

4.5 How does the number of spikes decrease?

In this section, we give a qualitative interpretation of how the number of spikes decrease when T_s and T_t are set with different values. When the same temperature is applied to the output logits of the teacher and the student, with the help of the softmax function as in Eq. 7, the *softened* output probabilities of the student are imitating the *softened* output probabilities of the teacher. Hence, the real student output probabilities are still sharp and deterministic, i.e., the output logits remain large in absolute values. As we already explained in Section. 4.3, large output logits means large number of spikes. However, when temperatures are applied individually to the output logits of the teacher and the student, we can control this distilling process. Especially when the temperatures of the student and the teacher are low and high, respectively, *hard* output probabilities of the student imitate the *softened* output probabilities of the teacher. This way, the teacher still gives rich knowledge to the student, since the temperature of the teacher remains high. Also, the real student output probabilities are more spread out, with the aid of low temperature. This means the range of the student output logits are reduced to small values. Since weights does not change much, from Eq. 2, we can expect that spikes will occur less to produce smaller outputs.

By performing a similar analysis as in Section. 4.3, but this time with the student SNN models with heterogeneous temperatures, we validate our claim. The weight distributions still do not show much difference, as in Fig. 5 (a) and (c). On the contrary, by examining the output distributions as in Fig. 5 (b) and (d), we can find a critical gap between the distributions. The outputs of the student SNN model trained with low T_s are condensed narrowly around zero.

The number of spikes keeps decreasing while maintaining accuracy when T_s is lowered to some extent. However, lowering T_s too much can instead hinder the accuracy improvement. For example, looking at Fig. 4 (a), $T_s = 1$ and $T_t = 8$ give the best accuracy, but when T_s was further reduced to 0.5 and to 0.1, the accuracy worsened. This could happen when the output logits of the students are excessively softened, making the boundary between the correct and wrong classes very ambiguous. Results with some extreme values of T_s and T_t are listed in Appendix B.

Table 2: Performance comparison with other SNN training methods on the MNIST dataset.

Method	Learning rule	Architecture	Time steps	Accuracy	Number of spikes
Diehl et al. 2015 [8]	C	CNN (3 layers)	200	99.10%	1.00E+05
Kim et al. 2018 [14]	C	CNN (3 layers)	16	99.20%	3.00E+06
Kheradpisheh et al. 2018 [13]	U	CNN (2 layers)	30	98.40%	6.00E+02
Park et al. 2019 [23]	C	CNN (3 layers)	87	99.25%	2.51E+05
Park et al. 2020 [24]	C	CNN (3 layers)	40	99.33%	2.00E+03
Lee et al. 2020 [17]	S	LeNet	50	99.59%	5.52E+04
Ours	S	CNN (3 layers)	10	99.43%	2.23E+04

4.6 Comparison with other methods

We compare the performance of the student SNN model distilled using our method to that of various other SNN training methods in Table. 2. For brevity of notation, in the learning rule column, we denote ANN-to-SNN conversion, unsupervised learning, and supervised learning as C, U, and S, respectively. As we can see in the table, the results by the conversion shows inefficiency in time steps and the number of spikes due to the lack of efficiency consideration during training. Unsupervised learning generates the smallest number of spikes but its training performance is lower than others. The other supervised learning [17] shows the highest test accuracy but it demands a large number of spikes on relatively large model (LeNet). Comparing other studies, our proposed approach achieves high accuracy with smaller number of spikes on a small SNN model. In addition, owing to the direct training through knowledge distillation, we also obtain the reduced inference latency.

5 Conclusion

In this work, we present a simple yet effective knowledge distillation method that considers the nature of SNNs. Existing studies that combined SNNs with knowledge distillation focused only on boosting the accuracy of the student SNN model, leaving the impact on the energy efficiency unexplored. To seek out this unknown impact, we first perform an exhaustive analysis on both inference accuracy and the number of spikes generated inside the networks, which is a good representative of energy efficiency. Through empirical analysis, we notice an undesirable situation in which the number of spikes escalated in high-accuracy student SNN models. Hence, we conduct another analysis on weight and output distributions of the distilled models to find out the cause and come up with a solution. By gathering intuitions from aforementioned consecutive experiments, we propose a novel energy-efficient knowledge distillation method to alleviate the problem of increasing spikes. This is done by simply separating the temperatures applied to student and teacher, which we call knowledge distillation with heterogeneous temperatures.

When we validated the proposed method with two standard datasets, the distilled student SNN model achieved additional increase in accuracy as well as reduction in the number of spikes. We explain how our method actually works by providing a qualitative interpretation with the analysis for validation. In the end, we compare the overall performance of our method with other training methods to highlight the strengths of our knowledge distillation with heterogeneous temperatures.

Since most of the studies related to knowledge distillation focuses on improving the performance of the student model, there are relatively few works that search the principles of the method itself, and this limitation also made us to take a passive attitude towards analyzing our method in a theoretical manner.

References

- [1] A. A. Al-Hamid and H. Kim. Optimization of spiking neural networks based on binary streamed rate coding. *Electronics*, 9(10):1599, 2020.
- [2] C. Buciluă, R. Caruana, and A. Niculescu-Mizil. Model compression. In *Proceedings of the 12th ACM SIGKDD international conference on Knowledge discovery and data mining*, pages 535–541, 2006.

- [3] T. Chen, I. Goodfellow, and J. Shlens. Net2net: Accelerating learning via knowledge transfer. *arXiv preprint arXiv:1511.05641*, 2015.
- [4] J. H. Cho and B. Hariharan. On the efficacy of knowledge distillation. In *Proceedings of the IEEE/CVF International Conference on Computer Vision*, pages 4794–4802, 2019.
- [5] S. S. Chowdhury, I. Garg, and K. Roy. Spatio-temporal pruning and quantization for low-latency spiking neural networks. *arXiv preprint arXiv:2104.12528*, 2021.
- [6] M. Davies, N. Srinivasa, T.-H. Lin, G. Chinya, Y. Cao, S. H. Choday, G. Dimou, P. Joshi, N. Imam, S. Jain, et al. Loihi: A neuromorphic manycore processor with on-chip learning. *IEEE Micro*, 38(1):82–99, 2018.
- [7] L. Deng, Y. Wu, Y. Hu, L. Liang, G. Li, X. Hu, Y. Ding, P. Li, and Y. Xie. Comprehensive snn compression using admm optimization and activity regularization. *arXiv preprint arXiv:1911.00822*, 2019.
- [8] P. U. Diehl, D. Neil, J. Binas, M. Cook, S.-C. Liu, and M. Pfeiffer. Fast-classifying, high-accuracy spiking deep networks through weight and threshold balancing. In *2015 International joint conference on neural networks (IJCNN)*, pages 1–8. ieee, 2015.
- [9] S. Han et al. Learning both weights and connections for efficient neural network. In *NIPS*, 2015.
- [10] S. Han et al. Deep compression: Compressing deep neural networks with pruning, trained quantization and huffman coding. In *ICLR*, 2016.
- [11] G. Hinton, O. Vinyals, and J. Dean. Distilling the knowledge in a neural network. *arXiv preprint arXiv:1503.02531*, 2015.
- [12] I. Hubara, M. Courbariaux, D. Soudry, R. El-Yaniv, and Y. Bengio. Quantized neural networks: Training neural networks with low precision weights and activations. *The Journal of Machine Learning Research*, 18(1):6869–6898, 2017.
- [13] S. R. Kheradpisheh, M. Ganjtabesh, S. J. Thorpe, and T. Masquelier. Stdsp-based spiking deep convolutional neural networks for object recognition. *Neural Networks*, 99:56–67, 2018.
- [14] J. Kim, H. Kim, S. Huh, J. Lee, and K. Choi. Deep neural networks with weighted spikes. *Neurocomputing*, 311:373–386, 2018.
- [15] Y. Kim and A. M. Rush. Sequence-level knowledge distillation. *arXiv preprint arXiv:1606.07947*, 2016.
- [16] R. K. Kushawaha, S. Kumar, B. Banerjee, and R. Velmurugan. Distilling spikes: Knowledge distillation in spiking neural networks. *arXiv preprint arXiv:2005.00288*, 2020.
- [17] C. Lee, S. S. Sarwar, P. Panda, G. Srinivasan, and K. Roy. Enabling spike-based backpropagation for training deep neural network architectures. *Frontiers in neuroscience*, 14, 2020.
- [18] S. Lu and A. Sengupta. Exploring the connection between binary and spiking neural networks. *Frontiers in Neuroscience*, 14:535, 2020.
- [19] W. Maass. Networks of spiking neurons: the third generation of neural network models. *Neural Networks*, 10(9):1659–1671, 1997.
- [20] F. Martinelli, G. Dellaerrera, P. Mainar, and M. Cernak. Spiking neural networks trained with backpropagation for low power neuromorphic implementation of voice activity detection. In *ICASSP 2020-2020 IEEE International Conference on Acoustics, Speech and Signal Processing (ICASSP)*, pages 8544–8548. IEEE, 2020.
- [21] P. Merolla et al. A million spiking-neuron integrated circuit with a scalable communication network and interface. *Science*, 345(6197):668–673, 2014.

[22] D. Neil, M. Pfeiffer, and S.-C. Liu. Learning to be efficient: Algorithms for training low-latency, low-compute deep spiking neural networks. In *Proceedings of the 31st annual ACM symposium on applied computing*, pages 293–298, 2016.

[23] S. Park, S. Kim, H. Choe, and S. Yoon. Fast and efficient information transmission with burst spikes in deep spiking neural networks. In *2019 56th ACM/IEEE Design Automation Conference (DAC)*, pages 1–6. IEEE, 2019.

[24] S. Park, S. Kim, B. Na, and S. Yoon. T2fsnn: deep spiking neural networks with time-to-first-spike coding. In *2020 57th ACM/IEEE Design Automation Conference (DAC)*, pages 1–6. IEEE, 2020.

[25] N. Rathi, P. Panda, and K. Roy. Stdp-based pruning of connections and weight quantization in spiking neural networks for energy-efficient recognition. *IEEE Transactions on Computer-Aided Design of Integrated Circuits and Systems*, 38(4):668–677, 2018.

[26] A. Romero, N. Ballas, S. E. Kahou, A. Chassang, C. Gatta, and Y. Bengio. Fitnets: Hints for thin deep nets. *arXiv preprint arXiv:1412.6550*, 2014.

[27] D. Roy, I. Chakraborty, and K. Roy. Scaling deep spiking neural networks with binary stochastic activations. In *2019 IEEE International Conference on Cognitive Computing (ICCC)*, pages 50–58. IEEE, 2019.

[28] B. Rueckauer, I.-A. Lungu, Y. Hu, M. Pfeiffer, and S.-C. Liu. Conversion of continuous-valued deep networks to efficient event-driven networks for image classification. *Frontiers in neuroscience*, 11:682, 2017.

[29] C. J. Schaefer and S. Joshi. Quantizing spiking neural networks with integers. In *International Conference on Neuromorphic Systems 2020*, pages 1–8, 2020.

[30] Y. Shi, L. Nguyen, S. Oh, X. Liu, and D. Kuzum. A soft-pruning method applied during training of spiking neural networks for in-memory computing applications. *Frontiers in neuroscience*, 13:405, 2019.

[31] S. B. Shrestha and G. Orchard. Slayer: Spike layer error reassignment in time. *arXiv preprint arXiv:1810.08646*, 2018.

[32] M. Sorbaro, Q. Liu, M. Bortone, and S. Sheik. Optimizing the energy consumption of spiking neural networks for neuromorphic applications. *Frontiers in neuroscience*, 14:662, 2020.

[33] E. Strubell, A. Ganesh, and A. McCallum. Energy and policy considerations for deep learning in NLP. In *ACL*, 2019.

[34] S. Sun, G. Cioffi, C. De Visser, and D. Scaramuzza. Autonomous quadrotor flight despite rotor failure with onboard vision sensors: Frames vs. events. *IEEE Robotics and Automation Letters*, 6(2):580–587, 2021.

[35] S. Takuya, R. Zhang, and Y. Nakashima. Training low-latency spiking neural network through knowledge distillation. In *2021 IEEE Symposium in Low-Power and High-Speed Chips (COOL CHIPS)*, pages 1–3. IEEE, 2021.

[36] T. Taunyazov, W. Sng, H. H. See, B. Lim, J. Kuan, A. F. Ansari, B. C. Tee, and H. Soh. Event-driven visual-tactile sensing and learning for robots. *arXiv preprint arXiv:2009.07083*, 2020.

[37] J. C. Thiele, O. Bichler, and A. Dupret. Spikegrad: An ann-equivalent computation model for implementing backpropagation with spikes. *arXiv preprint arXiv:1906.00851*, 2019.

[38] F. Tung and G. Mori. Similarity-preserving knowledge distillation. In *Proceedings of the IEEE/CVF International Conference on Computer Vision*, pages 1365–1374, 2019.

[39] Y. Wang, Y. Xu, R. Yan, and H. Tang. Deep spiking neural networks with binary weights for object recognition. *IEEE Transactions on Cognitive and Developmental Systems*, 2020.

- [40] J. Yim, D. Joo, J. Bae, and J. Kim. A gift from knowledge distillation: Fast optimization, network minimization and transfer learning. In *Proceedings of the IEEE Conference on Computer Vision and Pattern Recognition*, pages 4133–4141, 2017.
- [41] Y. Zhang, T. Xiang, T. M. Hospedales, and H. Lu. Deep mutual learning. In *Proceedings of the IEEE Conference on Computer Vision and Pattern Recognition*, pages 4320–4328, 2018.
- [42] H. Zheng, Y. Wu, L. Deng, Y. Hu, and G. Li. Going deeper with directly-trained larger spiking neural networks. *arXiv preprint arXiv:2011.05280*, 2020.

Appendix

A Detailed Experimental Settings

In this section, we describe the implementation details of the backpropagation process of SNNs, training hyperparameters, and the student SNN models used in this study. The functions, values, and network structures are carefully tuned to derive optimal results according to the MNIST and Fashion-MNIST datasets.

Surrogate gradient. A spike fires only when the membrane potential exceeds a certain threshold. This mechanism is implemented to experiments by setting the activation as a step function. Due to this non-differentiable spiking activity, which greatly hinders the learning of SNNs, we use a surrogate gradient to apply backpropagation. We approximate the Dirak delta function $\delta(u)$ to a rectangular function $h(u)$ expressed as follows:

$$h(u) = \begin{cases} d, & \text{if } |u - v_{\text{th}}| < \frac{1}{2d} \\ 0, & \text{otherwise,} \end{cases} \quad (\text{A1})$$

where d is a hyperparameter that determines the degree of approximation while maintaining the integral of $h(u)$ at 1. Several other forms of approximated functions were tested, but the above rectangular function gave the most satisfactory results.

Hyperparameter details. The types and values of hyperparameters used in the experiments are provided in Table. A1. Some hyperparameters are set to the same value regardless of the dataset. If the values are set differently depending on the dataset, values for the MNIST and Fashion-MNIST dataset are indicated outside and inside parentheses, respectively.

Table A1: Hyperparameters listed in alphabetical order.

Name	Value
batch size	1,000
degree of approximation	1
epoch	50 (100)
firing threshold	1
learning rate	1e-3
optimizer	Adam
time steps	10 (15)

Network structure details. Table. A2 shows the structures of the student SNN models for different datasets. 16C5 represents the convolution layer with 16 output channels and 5x5 filters. AP2 is the average-pooling layer with kernel size of 2, and FC10 is the fully connected layer with 10 output neurons.

Table A2: Detailed network structures for the MNIST and Fashion-MNIST datasets.

Dataset	Network structure
MNIST	16C5-AP2-64C5-AP2-FC10
Fashion-MNIST	32C3-AP2-64C3-AP2-FC128-FC10

B Complementary Results

Analyzing conventional knowledge distillation. Here we provide the actual numerical results on the MNIST and Fashion-MNIST dataset according to various configurations of T and α , as shown in Table. B1 and B2. For comparison, as also shown in the main experimental results, the baseline accuracy and the number of spikes are 99.14% and 28111 for the MNIST dataset and 90.98% and 79845 for Fashion-MNIST dataset, respectively.

Table B1: Accuracy (the number of spikes) on the MNIST dataset according to various configurations of T and α .

T	α				
	0.1	0.3	0.5	0.7	0.9
2	99.2% (40432)	99.18% (34805)	99.2% (35382)	99.17% (29541)	99.18% (29185)
4	99.28% (47873)	99.25% (49827)	99.27% (44078)	99.22% (35977)	99.15% (35434)
6	99.31% (56176)	99.29% (56071)	99.26% (50787)	99.24% (44654)	99.16% (43470)
8	99.34% (63184)	99.32% (61440)	99.28% (60610)	99.28% (53012)	99.24% (45608)

Table B2: Accuracy (the number of spikes) on the Fashion-MNIST dataset according to various configurations of T and α .

T	α				
	0.1	0.3	0.5	0.7	0.9
2	91.02% (102669)	91.06% (79396)	90.89% (80221)	90.89% (74898)	90.98% (73097)
4	91.46% (118904)	91.21% (111192)	91.25% (100405)	91.07% (77970)	90.83% (79118)
6	91.45% (117351)	91.39% (118702)	91.07% (116396)	91.08% (104063)	90.99% (91392)
8	91.41% (133702)	91.22% (132740)	91.08% (113767)	91.04% (99936)	90.84% (80705)

Weight distribution for all layers. As illustrated in Fig. B1, we present the normalized distributions of weights for all layers consisting the student networks. The distributions of the baseline, student trained with equal temperature, and student trained with heterogeneous temperature are colored blue, red and green, respectively.

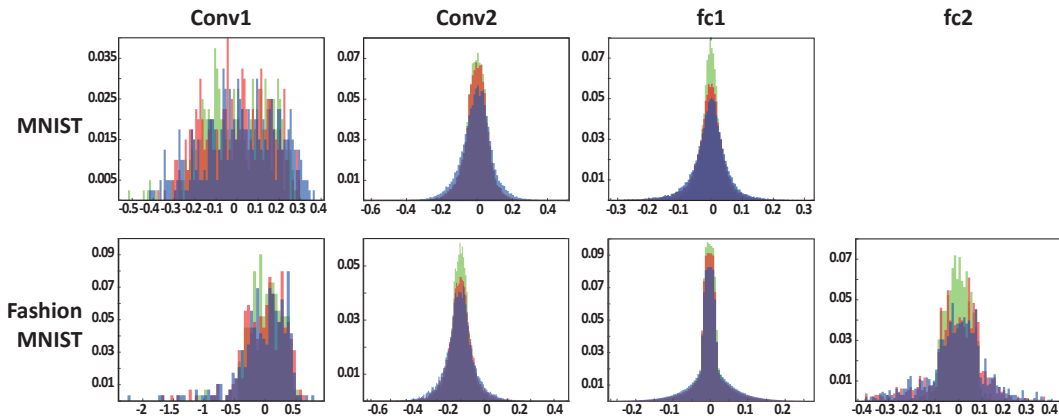


Figure B1: Normalized distributions for all layers of the student networks according to the MNIST and Fashion-MNIST datasets.

Layer-by-layer analysis of the frequency and the number of spikes. Here, we visualize how often and how many spikes fired per layer, measured from input to penultimate layer. The left and right column represents the results on the MNIST and Fashion-MNIST dataset, respectively. The top row

shows the spiking frequency of neurons per layer. The middle row shows the number of spikes per layer. The bottom row visualizes the number of spikes in another way such that it emphasizes how much the spikes generated in each layer accounted for the total number of spikes. For all layers and datasets, we can see that the spikes occurred most in the student with equal T and least in the student with heterogeneous T .

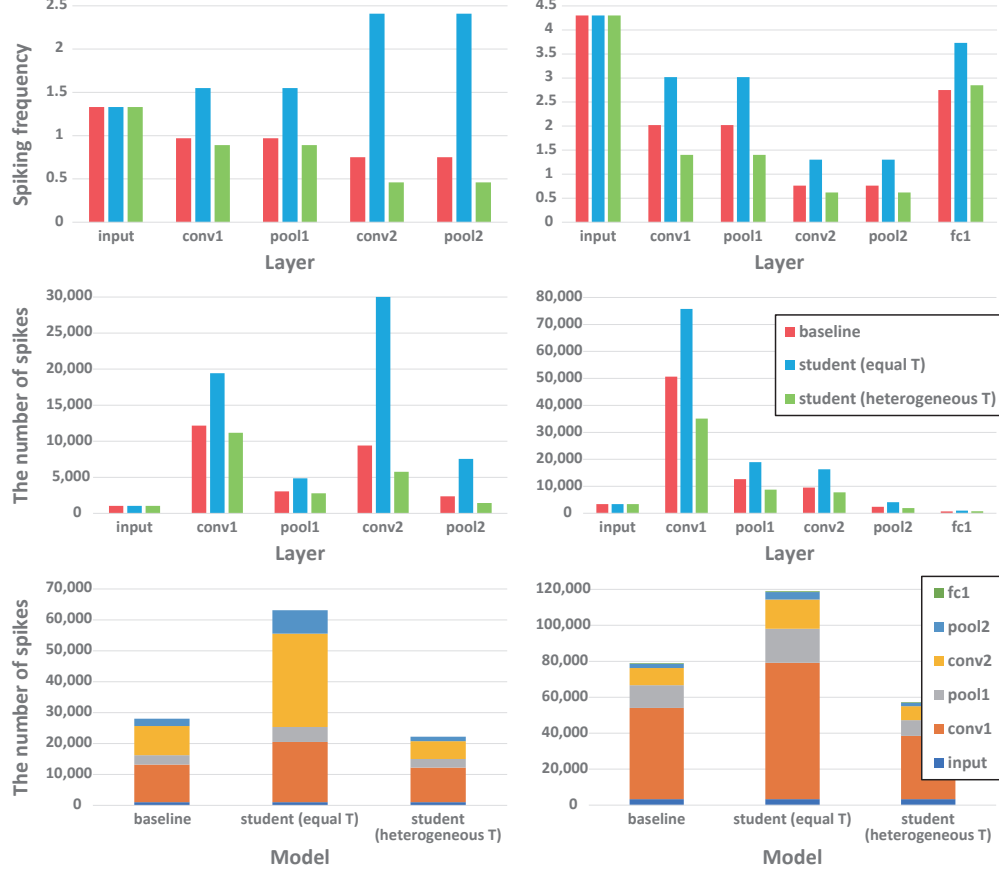


Figure B2: The frequency and the number of spikes per layer.

Using extreme values of T_s and T_t . We show that training with low T_s and high T_t gives a better performing student model. However, the performance of the student model starts to degrade when T_s and T_t go to extremes. Table. B3 shows some examples supporting this situation. It can be seen that the number of spikes is further reduced, but the accuracy also drops. When using our method, one should appropriately select temperatures considering the trade-off.

Table B3: Results using extreme values of T_s and T_t

T_s	T_t	Accuracy	Number of Spikes	Remarks
0.1	8	97.91%	9347	
0.2	8	98.64%	11488	very low T_s
0.5	8	99.32%	13393	
1	8	99.43%	22294	Reference
1	12	99.37%	16644	
1	16	99.36%	15290	very high T_t
1	20	99.33%	14338	